

钌多吡啶配合物与 DNA 作用及抗肿瘤活性

徐 丽^{*1} 陈 禹² 巫佳焕¹ 闻伴康¹

(¹ 广东药学院医药化工学院, 中山 528458)

(² 中山大学生命科学学院有害生物控制与资源利用国家重点实验室, 广州 510006)

摘要: 应用电子吸收光谱、荧光光谱和粘度测定等方法研究钌多吡啶配合物 $[\text{Ru}(\text{phen})_2(\text{Hecip})]_2$ (phen=1, 10-邻菲罗啉, Hecip=2-(9-乙基-9H-咪唑-3-基)-1H-咪唑并[4,5-f][1,10]菲罗啉) 与 DNA 相互作用。结果表明配合物与 DNA 键合计量比为 2:1, 键合常数超过 $10^5 \text{ mol}^{-1} \cdot \text{L}$, 配合物以插入方式与 DNA 结合。运用琼脂糖凝胶电泳实验研究配合物诱导 pBR322DNA 断裂及断裂机理。体外抗肿瘤活性结果表明配合物能有效抑制肿瘤细胞增殖, 进一步研究表明配合物可以将细胞周期阻滞在 S 期。

关键词: 钌配合物; 毒性; DNA 键合; 细胞周期阻滞

中图分类号: O614.82⁺1

文献标识码: A

文章编号: 1001-4861(2013)03-0613-08

DOI: 10.3969/j.issn.1001-4861.2013.00.107

DNA Interaction and Antitumor Activities of Ruthenium(II) Polypyridyl Complex

XU Li^{*1} CHEN Yu² WU Jia-Huan¹ WEN Ban-Kang¹

(¹ School of Chemistry and Chemical Engineering, Guangdong Pharmaceutical University, Zhongshan, Guangdong 528458, China)

(² State Key Laboratory of Biocontrol, Department of Biochemistry, College of Life Sciences, Sun Yat-Sen University, Guangzhou 510006, China)

Abstract: The interactions of the Ru(II) complex, $[\text{Ru}(\text{phen})_2(\text{Hecip})]^{2+}$ (phen=1,10-phenanthroline, Hecip=*N*-ethyl-4-([1,10]-phenanthroline [5,6-f]imidazol-2-yl)carbazole), with calf thymus DNA (CT DNA) were studied by using absorption spectroscopy, binding stoichiometry, viscosity measurement and photoactivated cleavage. A tight 2:1 complex is formed by the Ru(II) polypyridyl complex and CT DNA with a binding constant exceeding $10^5 \text{ mol}^{-1} \cdot \text{L}$ and with a binding mode of intercalation. Furthermore, the complex exhibits efficient DNA cleavage activity on UV (365 nm) irradiation via a mechanistic pathway involving formation of singlet oxygen as the reactive species. On the other hand, the cytotoxic activity of the complex was tested by 3-(4,5-dimethylthiazol-2-yl)-2,5-diphenyl-2H-tetrazolium bromide (MTT) method. The complex shows prominent anticancer activity against selected tumor cell lines with IC_{50} values lower than those of cisplatin. Further flow cytometry experiments show that the cytotoxic Ru(II) complex can cause cell cycle arrest in the S phase.

Key words: ruthenium complex; cytotoxicity; DNA-binding; cell cycle arrest

0 Introduction

Over the past few decades, Ru(II) complexes have been used as probes of DNA structure, artificial

nucleases, DNA molecular light switches and DNA photocleavage agents^[1-6]. Recently, their potential applications as cell imaging and anticancer agents have drawn much attention^[7-10]. Ruthenium complexes

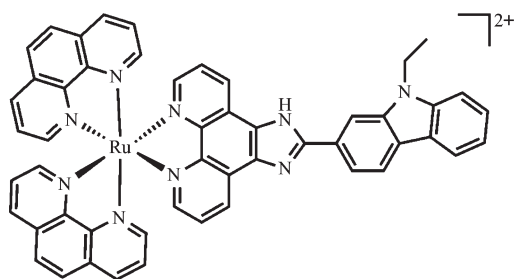
收稿日期: 2012-09-22。收修改稿日期: 2012-11-27。

2012 年广东省大学生创新创业训练计划(No.1057312013)资助项目。

*通讯联系人。E-mail: xuli473@163.com

are attractive alternatives to platinum-based anticancer agents and several ruthenium complexes have now been proposed as potential anticancer agents; such complexes can show remarkable anticancer activity and lower general toxicity than platinum compounds^[11-12]. These studies have stimulated much interest to investigate the bioactivities of ruthenium(II) complexes.

The carbazole group has attracted much interest in photoconductive^[13], photorefractive^[14], second-order nonlinear optical^[15], solar energy conversion^[16], and electroluminescent materials^[17] due to its excellent hole-transporting and donor properties. Wang and coworkers^[18-19] incorporated carbazole into the Ru^{II} complexes for DNA binding and pH- induced emission switching / sensing studies. In our previous work, we demonstrated that ruthenium(II) polypyridyl complex, [Ru(phen)₂(Hecip)]²⁺ (Scheme 1), could display fully reversible pH value controlled “on-off” luminescent signaling^[20]. To the best of our knowledge, however, little work has been devoted to the antitumor activity of the ruthenium complexes containing carbazole ligands. It is for this reason that we study the mode of DNA binding, cytotoxicity, cell cycle arrest of complex [Ru(phen)₂(Hecip)]²⁺. We demonstrate that the complex can intercalate between the base pairs of DNA. *In vitro* cytotoxicity assay shows that the complex exhibits cytotoxic potencies higher than that of cisplatin against the four human cancer cell lines screened. Further study shows that the complex inhibits cell growth through the induction of S phase cell cycle arrest.



Scheme 1 Structure of the complex

1 Experimental

1.1 Materials and methods

Calf thymus DNA (CT DNA) was obtained from

the Sino-American Biotechnology Company. pBR322 DNA was obtained from Shanghai Sangon Biological Engineering & Services Co., Ltd. Dimethyl sulfoxide (DMSO) was purchased from Sigma-Aldrich. Cell lines of HeLa (human cervical cancer cell line), MCF-7 (human breast adenocarcinoma cancer cell line), HepG2 (human hepatocellular liver carcinoma cell line) and A549 (human lung adenocarcinoma epithelial cell line) were supplied by Center of Experimental Animal Sun Yat-sen University (Guangzhou, China), agarose and ethidium bromide were obtained from Sigma-Aldrich. Doubly distilled water was used to prepare buffers (5 mmol·L⁻¹ Tris(hydroxymethylamino-methane)-HCl, 50 mmol·L⁻¹ NaCl, pH=7.2). A solution of calf thymus DNA in the buffer gave a ratio of UV absorbance at 260 and 280 nm of *ca.* (1.8~1.9):1, indicating that the DNA was sufficiently free of protein^[21]. The DNA concentration per nucleotide was determined by absorption spectroscopy using the molar absorption coefficient (6 600 mol⁻¹·L·cm⁻¹) at 260 nm^[22]. UV/Vis spectra were recorded on a Perkin-Elmer Lambda 850 spectrophotometer and emission spectra were recorded on a Perkin-Elmer LS 55 spectrofluorophotometer at room temperature.

1.2 DNA binding and photoactivated cleavage

All DNA binding experiments were performed in Tris-HCl buffer at 25 °C. The absorption titrations were performed using a fixed concentration (10 μmol·L⁻¹), to which the DNA stock solution was gradually added up to the point of saturation. Ru-DNA solutions were incubated for 5 min before the absorption spectra were recorded. The intrinsic binding constant *K_b* of the Ru(II) complex bound to DNA and the binding size *s* were calculated from the equation reported^[23].

Thermal denaturation studies were carried out with a Perkin-Elmer Lambda 850 spectrophotometer equipped with a Peltier temperature-controlling programmer (±0.1 °C). The temperature of the solution was increased from 40 to 95 °C at a rate of 1 °C·min⁻¹ and the absorbance at 260 nm was continuously monitored for solutions of CT-DNA (100 μmol·L⁻¹) in the absence and presence of the Ru(II) complex (10

$\mu\text{mol} \cdot \text{L}^{-1}$). The data are presented as $(A - A_0)/(A_f - A_0)$ vs temperature, where A , A_0 , and A_f are the observed, the initial, and the final absorbance at 260 nm, respectively.

Viscosity measurements were carried out using an Ubbelodthe viscometer maintained at a constant temperature at $(25.0 \pm 0.1)^\circ\text{C}$ in a thermostatic bath. DNA samples with approximately 200 base pairs in average length were prepared by Sonication^[24]. Flow time of each sample was measured three times, and an average flow time was calculated. Data were presented as $(\eta/\eta_0)^{1/3}$ versus binding ratio^[25].

For the gel electrophoresis experiment, supercoiled pBR322 DNA ($0.1 \mu\text{g}$) was treated with the Ru(II) complex in buffer, and the solution was then irradiated at room temperature with a UV lamp (365 nm, 10 W). The samples were analyzed by electrophoresis for 1.5 h at 80 V on a 0.8% agarose gel in TBE ($89 \text{ mmol} \cdot \text{L}^{-1}$ Tris-borate acid, $2 \text{ mmol} \cdot \text{L}^{-1}$ EDTA, pH = 8.3). The gel was stained with $1 \mu\text{g} \cdot \text{mL}^{-1}$ ethidium bromide and photographed on an Alpha Innotech IS-5500 fluorescence chemiluminescence and visible imaging system.

1.3 Continuous variation analysis

Binding stoichiometry was obtained for the complex with CT DNA using the method of continuous variation^[26]. The concentrations of the complex and DNA were varied, while the sum of the reactant concentrations was kept constant at $50 \mu\text{mol} \cdot \text{L}^{-1}$ (in terms of base pairs for the DNA). In the sample solutions, the molar fraction χ of complex was varied from 0 to 1.0 in 0.1 ratio steps. The fluorescence intensities of these mixtures were measured at 25°C using an excitation wavelength of 464 nm. The intensity in fluorescence was plotted versus the molar fraction χ of complex to generate a Job plot. Linear regression analysis of the data was performed in the software of Origin 7.0.

1.4 Cell culture and cytotoxicity assay *in vitro*

Standard 3-(4,5-dimethylthiazole)-2,5-diphenyltetraazolum bromide (MTT) assay procedures^[27] were performed using the methodology described in detail previously^[28]. Four different tumor cell lines were the

subjects of this study: HeLa, MCF-7, HepG2 and A549.

1.5 Cell cycle analysis

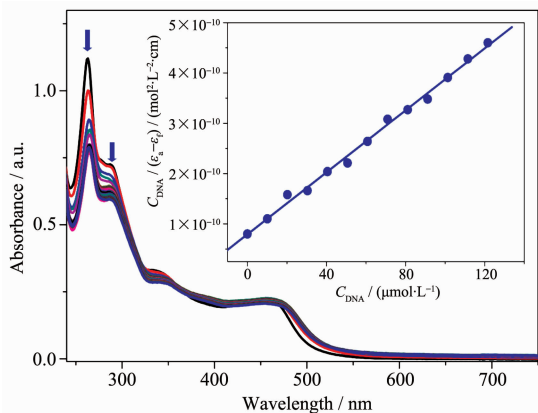
Cell Cycle analysis was performed as previously described^[11]. Briefly, HeLa cells were treated with Ru(II) complex ($10 \mu\text{mol} \cdot \text{L}^{-1}$) for various time intervals. The cells were harvested and fixed in 2 mL of 70% aqueous ethanol (V/V). After an incubation period of at least 12 h at -20°C , cells were washed with ice-cold PBS (Phosphate Buffered Saline). The cells were resuspended in 200 μL staining solution containing PI ($10 \mu\text{g} \cdot \text{mL}^{-1}$) and DNase-free RNase ($100 \mu\text{g} \cdot \text{mL}^{-1}$) and analyzed by a BD FACSCaliburTM cytometer (Becton Dickinson, Heidelberg, Germany). The number of cells analyzed for each sample was 10 000, and the experiments were repeated at least three times under identical conditions. Data were collected by BD CellQuestTM Pro software and analyzed by ModFit LT 2.0 software.

2 Results and discussion

2.1 Electronic absorption titration

In order to assess the DNA binding behavior of the complex, the absorption titration was carried out. As shown in Fig.1, with the increasing concentration of CT DNA, the electronic absorption spectra of the complex show no shift and little changes in the intensities for the charge transfer band at 464 nm. However, the band of the complex at 263 nm exhibits much more pronounced hypochromism of 29.88%. The large hypochromism observed may support an intercalative mode involving a strong stacking interaction between an aromatic chromophore and the base pairs of DNA. The intrinsic binding constant, which illustrates the binding strength of the complex with CT DNA, can be obtained by monitoring the changes in absorbance at 263 nm for the complex. The value of K for the complex is $(3.57 \pm 0.62) \times 10^5 \text{ mol}^{-1} \cdot \text{L}$ ($s = 2.12 \pm 0.35 \text{ bp}$ (base pair)). The K value is much larger than those of other typical DNA intercalative Ru(II) complexes ($1.1 \times 10^4 \sim 4.8 \times 10^4 \text{ mol}^{-1} \cdot \text{L}$)^[29], and is comparable to that of complexes $\Delta\text{-}[\text{Ru}(\text{phen})_2(\text{dppz})]^{2+}$ ($3.2 \times 10^5 \text{ mol}^{-1} \cdot \text{L}$) and $\Lambda\text{-}[\text{Ru}(\text{phen})_2(\text{dppz})]^{2+}$ (1.7×10^5

$\text{mol}^{-1} \cdot \text{L}$, dppz=dipyrido-[3,2-a-2',3'-c]phenazine^[30], but is not as strong as those of $[\text{Ru}(\text{phen})_2(\text{dppz})]^{2+}$ and $[\text{Ru}(\text{bpy})_2(\text{dppz})]^{2+}$ ($>10^6 \text{ mol}^{-1} \cdot \text{L}$), which are DNA intercalative Ru(II) complexes^[31]. The result suggests that the complex intercalatively binds to DNA, involving a strong stacking interaction between the aromatic chromophore and the base pairs of the DNA.

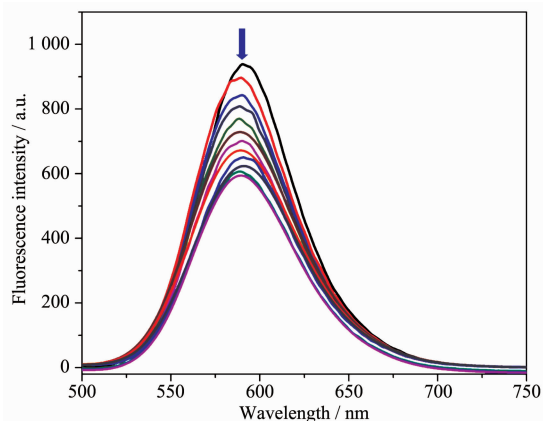


Arrow shows the absorbance change upon the increase of DNA concentration; Plots of $C_{\text{DNA}}/(\epsilon_s - \epsilon_t)$ versus C_{DNA} for the titration of DNA with Ru(II) complex

Fig.1 Absorption spectra of complex ($10 \mu\text{mol} \cdot \text{L}^{-1}$) in Tris-HCl buffer upon addition of CT-DNA

2.2 Luminescence studies

The complex can luminesce in Tris buffer at room temperature with a maximum appearing at 589 nm. Fig.2 shows the luminescence spectra of the complex in the absence and presence of increasing concentration of DNA in buffer solution. Upon



Arrow shows the intensity change upon increasing DNA concentrations

Fig.2 Emission spectra of complex ($10 \mu\text{mol} \cdot \text{L}^{-1}$) in Tris-HCl buffer in the absence and presence of CT-DNA

addition of DNA, the emission intensities increase to 1.46 times of the original intensities. The enhancement of emission intensity is an indication of binding of the complex to the hydrophobic pocket of DNA, and the complex can be protected efficiently by the hydrophobic environment inside the DNA helix.

2.3 Continuous variation analysis

Binding stoichiometry with CT DNA was also investigated through the luminescence-based Job plot (Fig.3). One major inflection point for the complex is observed at $\chi=0.64$. The data are consistent with a 2:1 $C_{\text{DNA}}/C_{\text{complex}}$ binding mode, suggestive of a specific Ru-CT DNA interaction.

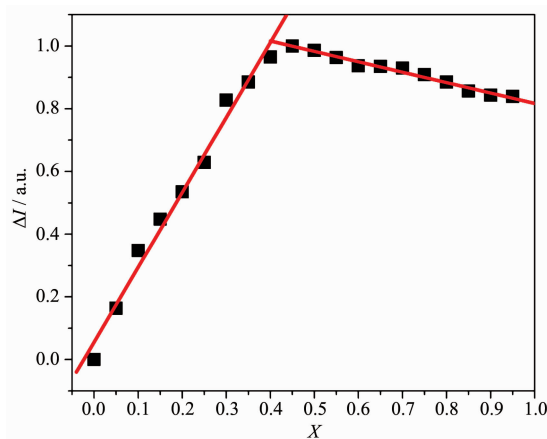


Fig.3 Job plot using luminescence data for complex with CT DNA in Tris-HCl buffer, pH=7.0, and X=molar fraction of complex added to DNA

2.4 DNA thermal denaturation studies

When the temperature in the solution increases, the double-stranded DNA gradually dissociates to single strands^[32], and generates a hyperchromic effect on the absorption spectra of DNA bases ($\lambda_{\text{max}}=260 \text{ nm}$). In order to identify this transition process, the melting temperature T_m , defined as the temperature where half of the total base pairs is unbonded, is usually introduced. According to previous literatures^[31,33], the intercalation of natural (or synthesized organics) and metallointercalators generally results in a considerable increase in melting temperature (T_m). The melting curves of CT-DNA in the absence and presence of the complex are presented in Fig.4. Here, The thermal denaturation experiment carried out for DNA in the absence of the Ru(II) complex reveals a T_m of (58.7 ± 0.3)

°C under our experimental conditions. The observed melting temperature in the presence of the complex is $(76.2 \pm 0.1)^\circ\text{C}$ at a concentration ratio of $r=0.10$ ($r=C_{\text{Ru}}/C_{\text{DNA}}$). The large increase in T_m of the Ru(II) complex (the ΔT_m is 17.5) is comparable to that observed for classical intercalators EB (13°C , $r=0.10$), Δ -[Ru(phen)₂(dppz)]²⁺ (16°C , $r=1$), and Λ -[Ru(phen)₂(dppz)]²⁺ (5°C , $r=1$)^[30]. The result also indicates the intercalative binding mode of [Ru(phen)₂(Hecip)]²⁺ to DNA.

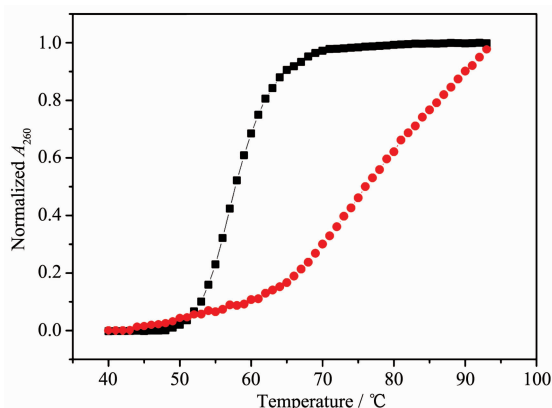


Fig.4 Thermal denaturation of CT-DNA in the absence (■) and presence of complex (●) $C_{\text{Ru}}=10 \mu\text{mol} \cdot \text{L}^{-1}$, $C_{\text{DNA}}=100 \mu\text{mol} \cdot \text{L}^{-1}$

2.5 Viscosity measurements

To further verify the interactions between the complex and CT-DNA, viscosity measurements were carried out. Viscosity measurements provide the most critical test for intercalative interaction^[34]. The effect of the Ru(II) complex together with EB (ethidium bromide) and [Ru(bpy)₃]²⁺ on the viscosity of CT DNA are shown in Fig.5. EB binds with DNA through the intercalation mode, whereas the [Ru(bpy)₃]²⁺ complex binds with DNA in the electrostatic mode, therefore the [Ru(bpy)₃]²⁺ complex exerts essentially no effect on DNA viscosity^[35]. On increasing the amount of Ru(II) complex, the relative viscosity of DNA increases steadily, which is similar to the behaviour of EB. The increased degree of viscosity, which may depend on the complex's affinity for DNA, follows the order of $\text{EB} > \text{Ru(II)} > [\text{Ru(bpy)}_3]^{2+}$. A similar sharp increase in relative viscosity has been observed on the addition of [Ru(bpy)₂(dppz)]²⁺, which was reported to be bound to DNA by intercalation. The results suggest that the Ru(II) complex binds to DNA through a classical

intercalation model. Such a result is consistent with the foregoing hypothesis.

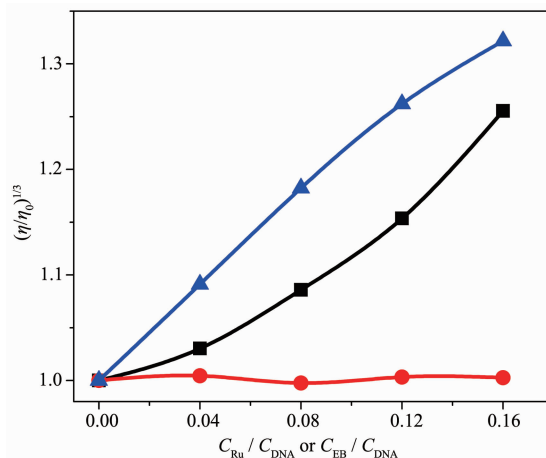
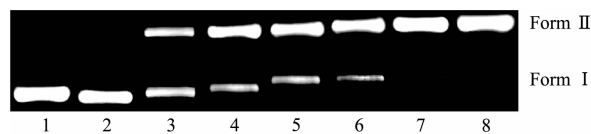


Fig.5 Effect of increasing amounts of complex (■), [Ru(bpy)₃]²⁺ (●) and EB (▲) on the relative viscosity of CT DNA at $(25 \pm 0.1)^\circ\text{C}$, $C_{\text{DNA}}=0.25 \text{ mmol} \cdot \text{L}^{-1}$

2.6 Photoactivated cleavage of pBR322 DNA

Fig.6a shows gel electrophoresis separation of pBR322 DNA after incubation with different concentrations of the Ru(II) complex upon irradiation at 365 nm for 30 min. No obvious DNA cleavage is observed for control (without complex, or incubation of the plasmid with the Ru(II) complex in darkness). As increasing the concentration of the complex, the amount of Form I (supercoiled form) of pBR322 DNA diminishes gradually, whereas that of Form II (circular form) increases. These results indicate that scission occurs on one strand (nicked).

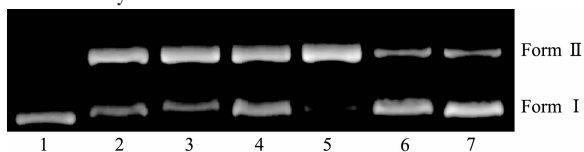


Lane 1: DNA control; Lane 2: DNA+complex ($5 \mu\text{mol} \cdot \text{L}^{-1}$); Lane 3~8: DNA+complex (5, 10, 15, 20, 30, 40 $\mu\text{mol} \cdot \text{L}^{-1}$), respectively

Fig.6a Photocleavage cleavage of pBR322 DNA in the absence and presence of different concentrations of Ru(II) complex after irradiation at 365 nm for 30 min

Fig.6b shows that the DNA cleavage of the plasmid by the complex is not inhibited in the presence of hydroxyl radical ($\cdot\text{OH}$) scavengers such as mannitol^[36] and dimethylsulfoxide (DMSO)^[37], which indicates that hydroxyl radical is not likely the

cleaving agent. In the presence of superoxide dismutase (SOD), a facile superoxide anion radical ($O_2^{\cdot-}$) quencher, the cleavage is obviously improved. The DNA cleavage of the plasmid is inhibited in the presence of the singlet oxygen (1O_2) scavenger histidine and NaN_3 ^[38-39], suggesting that 1O_2 is likely the reactive species responsible for the cleavage reaction. Related results of enhancement by SOD and inhibition by singlet oxygen scavengers have been observed by other ruthenium intercalators^[40-41].



Lane 1: DNA control; Lane 2: DNA+complex ($5 \mu\text{mol} \cdot \text{L}^{-1}$); Lane 3~7: DNA+complex ($5 \mu\text{mol} \cdot \text{L}^{-1}$)+Mannitol; DMSO; SOD; Histidine; NaN_3

Fig.6b Photocleavage of supercoiled pBR322 DNA by complex in the absence and presence of different inhibitors after irradiation at 365 nm for 30 min

2.7 Cytotoxicity assay *in vitro*

To explore the antitumor potential of the Ru(II) complex, HeLa, MCF-7, HepG-2 and A549 cells were treated with varying concentrations of Ru(II) for 48 h, and cell viability was determined by the MTT assay.

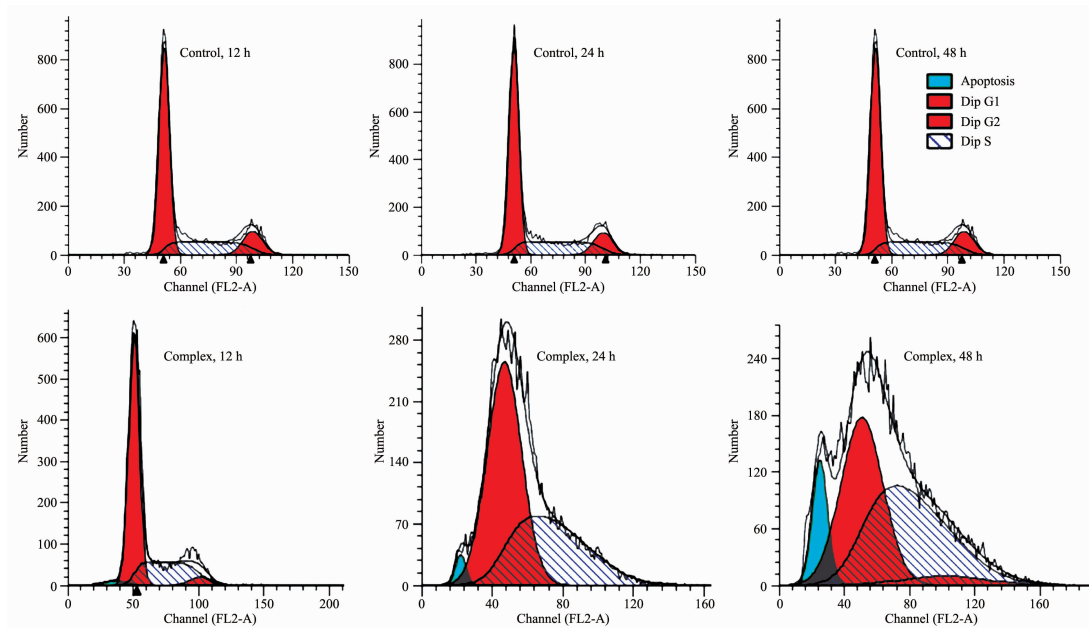
Cisplatin was used as a positive control. The resulting IC_{50} values for the tested complex are shown in Table 1. Based on the IC_{50} values, the complex has a significant inhibition to the growth and proliferation of all four tumor cells. Interestingly, the antiproliferative efficiency of the complex on the MCF-7 cells is much lower than that on the other three cell lines. The result also indicates that the complex is more potent than cisplatin against all the cancer cell lines screened. The cytotoxicity of the complex is higher than the other typical DNA intercalative Ru (II) complexes $[\text{Ru}(\text{phen})_2(\text{dppz})](\text{PF}_6)_2$ ^[12], $[\text{Ru}(\text{phen})_2(1\text{-Py-}\beta\text{C})](\text{PF}_6)_2$ ^[11] and $[\text{Ru}(\text{phen})_2(\text{mitatp})]^{2+}$ ^[42].

Table 1 IC_{50} values for complex against selected cell lines

Compound	$IC_{50} / (\mu\text{mol} \cdot \text{L}^{-1})$			
	HeLa	MCF-7	HepG2	A549
Complex	12.5 ± 1.2	33.3 ± 1.8	15.6 ± 0.8	9.4 ± 0.4
Cisplatin	16.5 ± 2.2	35.4 ± 4.4	20.2 ± 2.8	—

2.8 Cell cycle arrest

The cell cycle phase distribution of HeLa cells in response to Ru (II) treatment was studied by PI (propidium iodide) staining to further elucidate the mechanism of drug activity. Fig.7 shows the time dependent effect of the complex on cell-cycle



Dip G1: G0/G1 phase cells; Dip S: S-phase cells; Dip G2: G2/M-phase cells; apoptosis: apoptotic cells

Fig.7 Effect of complex ($10 \mu\text{mol} \cdot \text{L}^{-1}$) on the distribution of HeLa cells in cell cycle phases after treatment for 12, 24 and 48 h

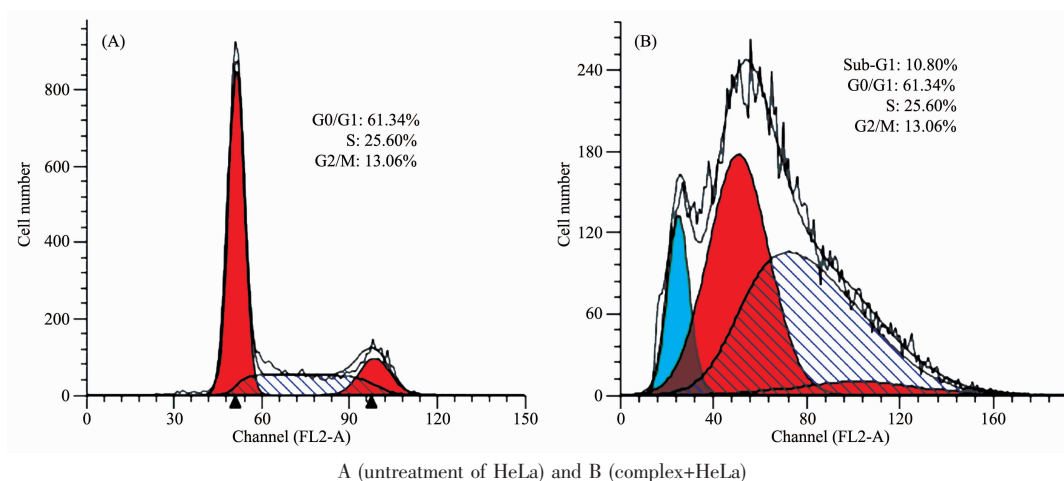


Fig.8 Cell cycle status of the HeLa cells after treatment with complex ($10 \mu\text{mol}\cdot\text{L}^{-1}$) for 48 h

distribution profiles with cells treated with vehicle (1% DMSO) as the control.

Cells in G0/G1 phase express a 2 N (diploid) DNA content, whereas cells in G2/M have a 4N (tetraploid) DNA content. DNA content of the cells in S phase is variable (between 2 N and 4 N). Sub-G1 fraction is usually indicative of degraded DNA and identified as a hallmark of apoptosis^[43]. Fig.8 shows the representative DNA distribution histograms of HeLa cell in the absence (A) and presence of the complex (B). Fig.8 shows that the treatment of HeLa cells with the complex, a large increase in the percentage of cell (%) at S phase and corresponding reduction at G0/G1 phase is observed, and a concomitant increase in the population of Sub-G1 phase cells is also observed, which suggests the antiproliferative mechanism on HeLa is S phase arrest.

3 Conclusions

The DNA-binding of the complex with CT DNA indicates that the complex can intercalate between DNA base pairs. The complex can effectively cleave plasmid DNA upon irradiated at 365 nm for 30 min. The studies of mechanism on photocleavage demonstrate that superoxide anion radical ($\text{O}_2^{\cdot-}$) and singlet oxygen ($^1\text{O}_2$) may play an important role. The data obtained from continuous variation analysis are consistent with a 2:1 $c_{\text{complex}}/c_{\text{DNA}}$ binding mode for the complex. The cytotoxicity assay indicates that the complex can inhibit the proliferation. The flow

cytometric analysis shows that treatment of HeLa cell with the complex indicates the induction of S phase arrest.

Acknowledgement: This work was supported by the Guangdong Pharmaceutical University.

References:

- [1] Greguric I, Aldrich-Wright J R, Collins J G. *J. Am. Chem. Soc.*, **1997**,**119**:3621-3622
- [2] Nair R B, Teng E S, Kirkland S L, et al. *Inorg. Chem.*, **1998**, **37**:139-141
- [3] Erkkila K E, Odom D T, Barton J K. *Chem. Rev.*, **1999**,**99**: 2777-2796
- [4] Friedman A E, Chambron J C, Sauvage J P, et al. *J. Am. Chem. Soc.*, **2004**,**126**:8630-8631
- [5] Zeglis B M, Barton J K. *J. Am. Chem. Soc.*, **2006**,**128**:5654-5655
- [6] Liu Y, Hammitt R, Lutterman D A, et al. *Inorg. Chem.*, **2007**, **46**:6011-6021
- [7] Cosgrave L, Devocelle M, Forster R J, et al. *Chem. Commun.*, **2010**,**46**:103-105
- [8] Tan C P, Wu S H, Lai S S, et al. *Dalton Trans.*, **2011**,**40**: 8611-8621
- [9] Tan L F, Shen J L, Liu J, et al. *Dalton Trans.*, **2012**,**41**:4575-4587
- [10] Liu Y J, Li Z Z, Liang Z H, et al. *DNA Cell Biol.*, **2011**,**30**: 839-848
- [11] Tan C P, Lai S S, Wu S H, et al. *J. Med. Chem.*, **2010**,**53**: 7613-7624
- [12] Schatzschneider U, Niesel J, Ott I, et al. *ChemMedChem*, **2008**,**3**:1104-1109

- [13]Van Dijken A, Bastiaansen J J A M, Kiggen N M M, et al. *J. Am. Chem. Soc.*, **2004**,**126**:7718-7727
- [14]Grabowski Z R, Rotkiewicz K. *Chem. Rev.*, **2003**,**103**:3899-4032
- [15]Zhang Y, Wang L, Wada T, et al. *Macromol. Chem. Phys.*, **1996**,**197**:1877-1888
- [16]Wagner J, Pielichowski J, Hinsch A, et al. *Synth. Met.*, **2004**,**146**:159-165
- [17]Xin H, Sun M, Wang K Z, et al. *Chem. Phys. Lett.*, **2004**, **388**:55-57
- [18]Liu F R, Wang K Z, Bai G Y, et al. *Inorg. Chem.*, **2004**,**43**: 1799-1806
- [19]Lü Y Y, Gao L H, Han M J, et al. *Eur. J. Inorg. Chem.*, **2006**,**430**:430-436
- [20]Xu L, Liu P X, Liao G L, et al. *Aust. J. Chem.*, **2010**,**63**:1-9
- [21]Marmur J A. *J. Mol. Biol.*, **1961**,**3**:208-218
- [22]Reichmann M E, Rice S A, Thomas C A, et al. *J. Am. Chem. Soc.*, **1954**,**76**:3047-3053
- [23]Wolf A, Shimer Jr G H, Meehan T. *Biochemistry*, **1987**,**26**: 6392-6396
- [24]Chaires J B, Dattagupta N, Crothers D M. *Biochemistry*, **1982**,**21**:3933-3940
- [25]Cohen G, Eisenberg H. *Biopolymers*, **1969**,**8**:45-55
- [26]Job P. *Ann. Chim.*, **1928**,**9**:113-203
- [27]Mosmann T. *J. Immunol. Methods.*, **1983**,**65**:55-63
- [28]Tan L F, Song F C, Zou X Q, et al. *DNA Cell Biol.*, **2011**, **30**:277-285
- [29]Pyle A M, Rehmann J P, Meshoyrer R, et al. *J. Am. Chem. Soc.*, **1989**,**111**:3051-3058
- [30]Han M J, Duan Z M, Wang K Z, et al. *J. Phys. Chem. C.*, **2007**,**111**:16577-16585
- [31]Friedman A E, Chambron J C, Sauvage J P, et al. *J. Am. Chem. Soc.*, **1990**,**112**:4960-4962
- [32]Tselepi-Kalouli E, Katsaros N. *J. Inorg. Biochem.*, **1989**,**37**: 271-282
- [33]Liu J G, Zhang Q L, Shi X F, et al. *Inorg. Chem.*, **2001**,**40**: 5045-5050
- [34]Satyanarayana S, Dabrowiak J C, Chaires J B. *Biochemistry*, **1992**,**31**:9319-9324
- [35]Satyanarayana S, Daborusak J C, Chaires J B. *Biochem.*, **1993**,**32**:2573-2584
- [36]Cheng C C, Rokita S E, Burrows C J. *Angew. Chem. Int. Ed. Engl.*, **1993**,**32**:277-278
- [37]Lesko S A, Lorentzen R J, Ts'o P O. *Biochemistry*, **1980**,**19**: 3023-3028
- [38]Nilsson R, Merkel P B, Kearns D R. *Photochem. Photobiol.*, **1972**,**16**:117-124
- [39]Patra A K, Nethaji M, Chakravarty A R. *J. Inorg. Biochem.*, **2007**,**101**:233-244
- [40]Deshpande M S, Kumbhar A A, Kumbhar A S, et al. *Bioconjugate Chem.*, **2009**,**20**:447-459
- [41]Gao F, Chao H, Ji L N. *Chem. Biodivers.*, **2008**,**5**:1962-1979
- [42]Yu H J, Chen Y, Yu L, et al. *Eur. J. Med. Chem.*, **2012**,**55**: 146-154
- [43]Karna P, Sharp S M, Yates C, et al. *Mol. Cancer.*, **2009**,**8**: 93